Influence of Cloud and Solar Zenith Angle on the Diffuse Solar Erythemal UV Short Wavelength Cut-offs and Maximum Spectral Irradiance Wavelengths

Alfio V. Parisi[1,*], David J. Turnbull[1], Chris de Byl[1], Peter Schouten[1], Joanna Turner[1] and Nathan Downs[1]

[1]Faculty of Sciences, University of Southern Queensland, TOOWOOMBA. 4350. AUSTRALIA. Fax: 61 74 6312721.

[*]Corresponding author email: **parisi@usq.edu.au** (Alfio V. Parisi)

Abstract

Cloud and the solar zenith angle (SZA) influence the magnitude of the diffuse erythemal UV. The aim of this research was to investigate the variation of the short wavelength cut-off and the maximum spectral irradiance wavelength for the diffuse spectral erythemal UV. The diffuse spectral solar UV was measured on a horizontal plane at ten minute intervals over a four month period with a UV spectroradiometer for the SZA range of 4.1^{o} to 80^{o}. The short wavelength cut-offs and the maximum spectral irradiance wavelengths of the diffuse erythemal UV did not change significantly with cloud cover. The short wavelength cut-off was influenced by SZA and ranged from 290.5 ± 0.3 nm for the small SZA to 295.1 ± 0.7 nm for the larger SZA. The maximum spectral irradiance wavelength of the diffuse erythemal UV was not influenced significantly for SZA of 40^{o} or less. For higher SZA, the maximum spectral irradiance wavelength of the diffuse erythemal UV increased from 305 nm to 313.9 nm.

Introduction

The global solar UV radiation incident on a receiving plane is comprised of the direct part that arrives in a direct path from the sun and the diffuse part that is scattered by environmental and atmospheric components and as a result is incident from all directions. As the solar zenith angle (SZA) increases the relative proportion of diffuse UV in the global solar UV also increases (1). Of the total received global UV, the diffuse UV possesses a higher proportion of the shorter wavelengths compared to the direct solar UV. These shorter wavelengths also correspond to the higher relative effectiveness of the respective action spectra for skin and eye damage (2,3).

The diffuse UV also forms a significant percentage of the UV exposures to parts of the population that are in shade, for example tree shade (4) or the shade of different structures (5). Similarly, for parts of the face protected from the direct UV component by hats, the UV exposure to these parts is due to the diffuse UV component. Diffuse UV radiation can be influenced by surrounding structures in the form of reflection, although only certain types of surfaces will significantly influence total UV radiation (6,7) such as metal sheeting. In general the significant influence is from direct UV radiation incident on a surface, which when reflected, can contribute an increase in the diffuse component of UV radiation.

The diffuse solar UV has been recorded in a number of monitoring programs. An example of this is the USDA ultraviolet monitoring program (8) where a network of broadband sensors, each fitted with seven narrow band filters allows measurement of the UV irradiances at those seven wavelengths. A rotating shadow band is employed to measure the global and diffuse UV. Measurement of the global and diffuse UV spectrum

has been undertaken at a high southern latitude employing a shadow band fitted to a Biospherical Instruments GUV-511 filter instrument and the total ozone values calculated from the derived direct spectral UV radiation (9). The shadow bands fitted to UV measuring instruments obscure a small part of the sky and it is possible to determine and correct for this by determining the shadow band correction. Grant (10) developed a method to correct for the shadow band in the case of the photosynthetic radiation, based on modelling of the distribution of the radiation in this waveband. Rosales et al. (9) has presented a technique to calculate the shadow band correction employing the measurements of four spectra with the shadow band at different angles over a short period. Brewer spectrophotometers measure the direct and global UV spectral irradiances from which the diffuse spectral UV can be calculated (11). The direct solar UV is measured by directing the optics to the solar disc. Grant and Gao (12) developed a model to calculate the diffuse fraction of the UVA and UVB for partly cloudy skies.

Strategies to minimize personal UV exposure have been widely promoted (12). These strategies are encouraged in skin cancer prevention campaigns in order to reduce the risks of keratinocyte carcinoma, cutaneous malignant melanoma and sun-related disorders later in life. General guidelines exist for the provision of shade (13-17). Various studies have shown that damaging UV exposure is possible under shade structures due to diffuse UV radiation (18,19). In order to reduce the exposures to diffuse UV radiation, further quantitative research is required to provide a better understanding of the diffuse solar UV environment. The influencing factors on the solar UV spectrum are primarily the angle of the sun, clouds, ozone and aerosols. A knowledge of the short wavelength cut-off is important as the action spectra for biologically damaging UV exposures increases in effectiveness at the shorter wavelengths, and the variation in short wavelength cut-off can

be used to describe the quality of the biologically damaging UV spectrum as used by Kollias et al., (20). The short wavelength cut-off is the wavelength at which the spectral irradiance starts to become distinguishable from the background noise of the measuring spectroradiometer and is the minimum wavelength at which terrestrial solar UV takes effect. This wavelength cut-off is not necessarily the minimum measured wavelength of a weighting function, which may extend outside the solar UV radiation waveband. The variation of the short wavelength cut-off of the global erythemally weighted solar UV spectrum (20) and the spectral biologically damaging UV for cataracts on a horizontal plane (21) have been investigated. Kollias et al., (20) also records the most maximally effective wavelength of the biologically damaging UV global spectrum, which is an effective way to describe the intensity of the biologically damaging UV spectrum. In this paper this maximally effective wavelength is described as the maximum spectral irradiance wavelength. A research question generated from this research that will be investigated in this paper is how does the short wavelength cut-off of the diffuse erythemal UV spectral irradiance and the maximum spectral irradiance wavelength of the diffuse erythemal spectral UV vary with SZA and with cloud cover.

Materials and methods

Diffuse UV spectrum

Diffuse solar UV spectral data from 280 to 400 nm in 0.5 nm steps has been collected in ten minute intervals at Toowoomba (27.6^{o} S, 151.9^{o} E, 693 m above sea level), Australia. The spectral instrument has a double grating monochromator with 2400 lines mm^{-1} and a bandwidth of 0.5 nm (model DTM300, Bentham Instruments, Reading, UK). A small variation in the bandwidth of the instrument may have an impact on the resulting diffuse UV irradiance, however this is within the overall error of the spectroradiometer which is

discussed later in this paper. The instrument is mounted in an air-tight container on the roof of a building with unobstructed sky views. Details of the instrument have been previously provided (22). The input optics of this instrument is a diffuser with a cosine error of ±0.8% for SZA up to 70° and 3.3% for SZA of 80°. In general, despite the poor cosine response at larger SZA, measurement of UV radiation using a diffuser is reasonable due to the large proportion of scattered (diffuse) UV radiation in the atmosphere. The non-angular dependence of the diffuse UV can reduce the effect of the error of the cosine response, which is angular dependent.

An automatic rotating shadow band (model RSB, Bentham Instruments, Reading, UK) that is 15 mm wide and 110 mm above the spectroradiometer input optics was employed for the collection of the spectral diffuse UV data. This shadow band rotates into position to block the solar disc from the input optics for the collection of the diffuse UV spectrum and rotates to a position in the horizontal plane for the recording of the global UV spectrum. The configuration of the shadow band over the sensor is shown in Figure 1. Control of the instrumentation is provided by the BenWin+ software (version 1.0.4.13, Bentham Instruments, Reading, UK). The software contains a sun tracking module that employs the position of the site and the date and time of day to calculate the position of the sun and the angle above the horizontal plane that the band has to be positioned in order to block the sun and moves the shadow band accordingly. Communication between the control computer in the laboratory and the spectroradiometer and the rotating shadow band controller on the roof is via a GPIB-ENET/100 controller (model GPIB-ENET/100, National Instruments) connected to the network.

The software is configured to start scanning at 5:00 EST (Australian Eastern Standard Time), with the last scan for the day at 19:00 EST. The recording of the diffuse UV spectra starts at each of hh:05, hh:15, hh:25, hh:35, hh:45 and hh:55 and the recording of the global UV spectra starts at each of hh:00, hh:10, hh:20, hh:30, hh:40 and hh:50 where hh is the hour of the day between 5:00 EST and 19:00 EST. The time taken to collect a spectrum is approximately one minute. This results in the collection of six diffuse UV spectra and six global UV spectra every hour. The software corrects for the dark count of each spectrum that is recorded prior to the start of each scan. This initialisation process for each scan takes approximately one minute and for each scan it starts one minute prior to the start of each scan.

The period of data collection was in the Southern Hemisphere late spring and summer from 1 November 2006 to 28 February 2007. The minimum SZA in this period was 4.1^{o} In this research, data with SZA up to 80^{o} were employed. The container in which the spectroradiometer is housed is temperature stabilised with a Peltier system and the temperature set to 25 ^{o}C. The temperature inside the container at each scan is recorded by the software. For the times that the temperature inside the container housing the spectroradiometer varied by more than 1 ^{o}C from the set temperature due to hot ambient temperatures, the manufacturer supplied temperature correction factor of -0.4%/^{o}C was applied in the post processing to the spectral irradiance data collected at each 0.5 nm increment. This correction was the same at all wavelengths. The wavelength shift of the instrument due to temperature as provided by the manufacturer is 0.005 nm/^{o}C. Consequently, any wavelength shift was minimal and no correction for wavelength shift has been applied. The uncertainty of the spectral UV data was of the order of ±6% (not

including ±3% uncertainty in the traceability of the calibration lamp to the UK standard) (22).

The correction due to the shadow band has been determined with the technique described by Rosales et al. (9) where the spectral irradiances were measured with the shadow band on the horizontal plane for a global scan, with the shadow band shading the sensor for a diffuse scan and with the shadow band at an angle of 13^o to the east of the position where it shaded the sensor and at an angle of 13^o to the west of the position where it shaded the sensor. The angle of 13^o was employed as that is the angle used in the previous research (9). This angle is such that the input sensor is not shaded by the shadow band and the shadow provided by the shadow band is first to one side of the sensor and then to the other side. The sequence took approximately a total of nine minutes to allow positioning of the band and record the spectra at all four positions of the band. Any change in the angle of the sun during this time would have been minimal. Each series of four measurements were repeated for a series of times between 8:08 EST and 16.51 EST over two days to determine the average correction factor for the shadow band. Each sequence of scans was performed when the sky was mainly clear of cloud with the cloud cover being less than 4% on all of the scans as calculated from the Total Sky Imager. The measurement site has skies with predominantly low aerosol content and there would have been minimal change in the influence due to aerosols over the two consecutive days. The values of the spectral irradiances at each 0.5 nm increment for each scan were multiplied by this correction factor.

Each UV spectrum was weighted with the erythemal action spectrum (2) to produce the diffuse spectral erythemal UV at each time. The process for the calculation of the short

wavelength cut-off was to determine the maximum of the spectral erythemal UV and the short wavelength cut-off was taken as the wavelength at which the spectral erythemal UV was 0.1% of the maximum for that spectrum (21). Previous research has employed the wavelength at which the irradiance was 1% of the maximum irradiance for that scan (20) and also the wavelength at which the irradiance was 0.1% of the maximum irradiance for that scan (21). In this current research, the diffuse erythemal UV still had a significant irradiance at 1% of the maximum irradiance. Based on this, the short wavelength cut-off was defined as the wavelength at which the erythemal UV spectral irradiance was 0.1% of the maximum erythemal spectral irradiance for that scan.

The amount of cloud cover at the time of each UV spectral scan was quantified by a Total Sky Imager (TSI) (model TSI-440, Yankee Environmental Systems, MA, USA) that is installed on the same building roof and several metres from the UV spectroradiometer. This instrument and associated software package allows determination of the fractional cloud cover at one minute intervals. Each tenth image coincides with the time of the start of a spectral UV scan. The software also provides the SZA at each five minute point when the cloud cover is determined. The cases with less than 2% cloud cover were classified as cloud free. The error in the determination of the amount of cloud cover is approximately ±10% (23). Over the four month period, the average of the total column ozone from the OMI satellite (23) on each day was 274 DU with minimum and maximum values of 244 DU and 311 DU.

Results

Diffuse UV spectrum

A typical diffuse UV solar spectrum for an SZA of 5.4^{o} and the associated spectral erythemal UV is shown in Figure 2. For comparison, the corresponding global UV

spectrum and associated erythemal UV is also shown. The Fraunhofer spectral lines present in the global spectrum are also present in the diffuse spectrum. From the figure, it can be seen that the relative proportion of the spectral diffuse UV to the global UV is higher in the UVB waveband than in the UVA waveband. This is due to the scattering of UVB wavelengths, which scatter more easily than UVA wavelengths. The proportion of diffuse UVB to direct UVB is much greater than the proportions of diffuse UVA to direct UVA throughout the day due to this characteristic feature. For these example spectra, the percentage of the diffuse UV to global UV at 310 nm is 48% compared to 31% at 370 nm. These percentages at these wavelengths will change for different SZA, ozone levels and for the cases with cloud cover (24). For an SZA of 46^{o} on the same day, the ratio of the spectral diffuse UV to the global UV is 70% at 310 nm and 52% at 370 nm.

The diffuse erythemal UV irradiances calculated from the spectral diffuse UV for the two days on 15 November 2006 (day 319) and 21 November 2006 (day 325) with the first being cloudy and the second one being cloud free are shown in Figure 3. For the first day, the cloud fraction ranged from 1 to 0.1. On the second day, the cloud fraction was less than 2% for all of the day except for one five minute point when it was measured as 6%. The total column ozone from the OMI satellite (25) on each day is 296 DU and 284 DU respectively. The data is shown at 10 minute intervals, except for any small intervals where there was no data collected. The scatter of the data is higher on the cloudy day, however the peak in the diffuse erythemal UV irradiances are higher on the cloudy day due to the higher proportion of scattering on the cloudy day. The peak in the diffuse erythemal irradiance is higher by a factor of 1.31 for the cloudy day compared to the clear day with the peak diffuse irradiances of 188.4 mW m^{-2} and 143.4 mW m^{-2} for the cloudy day and the clear day respectively.

Short wavelength cut-off

For the same two days, the variation in the short wavelength cut-off of the diffuse erythemal UV with time of day is shown in Figure 4 for the cloudy day (day 319) and the cloud free day (day 325). Although, the spectral diffuse erythemal irradiances are different on the two days, there is no noticeable difference between the two days in the variation throughout the days for the cut-off wavelength. The shortest cut-off wavelengths are 291 nm and 290.5 nm on the days. A Student's two sample t-test was employed to test for statistically significant differences in the cut-off wavelengths between the two days. This produced a value of 0.16 that shows that there is no significant difference in the cut-off wavelengths on the cloudy and clear days.

The short wavelength cut-off variation of the diffuse erythemal spectral UV with SZA is shown in Figure 5 for all cases and for the cases of cloud free skies. There are 2,146 cloud free cases compared to the total of 5,598 for all sky conditions. Each data point is the average over the four months of data of the cut-off wavelengths for the range of SZA that are 5° either side of the data point. The error bars are ± one standard deviation of the values in this range. The cut-off wavelength for erythemal UV increases with SZA from 290.5 nm to 295.1 nm for 10^o to 70^o. For higher SZA, the mean drops slightly from 295.1 nm to 294.7 nm for SZA of 70^o to 80^o for part (a) and from 295 nm to 294.7 nm for the cloud free cases, however in both cases it is still within the error bar range of the value for 70^o.

Maximum spectral irradiance wavelength

The wavelengths at which the maximum spectral diffuse erythemal irradiances occur for the range of SZA are shown in Figure 6. Each data point is the average over the four months of the data that are 5^o either side of the data point and the error bars are ± one standard deviation of the values in this range. For SZA up to and including 40^o, the wavelength at which the maximum occurs is unchanged at 305 nm. For larger SZA, the wavelength for the maximum shifts to longer wavelengths due to the increased ozone absorption at the shorter wavelengths resulting from the longer path of the radiation through the atmosphere. The maximum spectral irradiance wavelength for the cloud free cases were considered and the averages at each 10^o increment of SZA were within 0.4 nm or less of the averages for the cases of all cloud conditions.

Discussion

The diffuse component of the solar UV forms a significant proportion of the UV exposures to the population during normal daily activities and an even higher proportion during activities in shaded or partly shaded environments. The short wavelength cut-off and wavelength with the maximum spectral irradiance of the global erythemally weighted solar UV spectrum (20) and the spectral biologically damaging UV for cataracts on a horizontal plane (21) have been previously investigated. This paper has extended this previous research to investigate the variation due to SZA and cloud cover of the short wavelength cut-off and the maximum spectral irradiance wavelength for the diffuse spectral erythemal UV on a horizontal plane.

The results show that the short wavelength cut-off of the diffuse erythemal UV throughout the day and over the four month period is not influenced by cloud. Similar results have been reported on the influence of cloud on the global erythemal UV (20). For

the clouds present during November 2006, there is some influence to the value of the maximum spectral irradiance wavelength of the diffuse erythemal UV, however there is no significant influence due to clouds to the wavelength at which maximum spectral irradiance occurs. Of the two factors of clouds and SZA investigated in this research, SZA influences the short wavelength cut-off for the diffuse erythemal UV spectrum. This variation of the short wavelength cut-off for diffuse erythemal UV is only 5 nm over the SZA range. The SZA also influences the maximum spectral irradiance wavelength for diffuse erythemal irradiances, but only for SZA above 40°. Therefore, the short wavelength cut-off and maximum spectral irradiance wavelength are influenced more significantly by SZA than cloud cover.

ACKNOWLEDGEMENTS: *The UV spectroradiometer was funded by the Australian Research Council. The authors acknowledge USQ technical staff for assistance in setting up the spectroradiometer and Dr Jeff Sabburg for the TSI data.*

References

1. Blumthaler, M. and Ambach, W., "Spectral measurements of global and diffuse solar ultraviolet-B radiant exposure and ozone variations", *Photochem. Photobiol.* (1991), **54**, 429-432.
2. CIE (International Commission on Illumination), "A reference action spectrum for ultraviolet induced erythema in human skin", *Comm. Int. Eclairage J*. (1987), **6**, 17-22.
3. Oriowo, O.M., Cullen, A.P., Chou, B.R. and Sivak, J.G., "Action spectrum and recovery for *in vitro* UV-induced cataract using whole lenses", *Ophthalmol. Visual. Sci.,* (2001), **42**, 2596-2602.
4. Parisi, A.V., Kimlin, M.G., Wong, J.C.F. and Wilson, M., "Diffuse component of the solar ultraviolet radiation in tree shade", *J. Photochem. Photobiol. B: Biol.* (2000), **54**(2-3), 116-120.
5. Turnbull, D., Parisi, A.V. and Sabburg, J., "Scattered UV beneath public shade structures during winter", *Photochem. Photobiol.* (2003), **78**(2), 180-183.
6. Turner, J., Parisi, A.V. and Turnbull, D.J., "Reflected solar radiation from horizontal, vertical and inclined surfaces: Ultraviolet and visible spectral and broadband behaviour due to solar zenith angle, orientation and surface type", *J. Photochem. Photobiol. B. Biol.* (2008), **92,** 29-37.
7. Turner, J. and Parisi, A.V., "Measuring the influence of UV reflection from vertical metal surfaces on humans", *Photochem. Photobiol. Sci.,* (2008), **8**, 62-69.
8. Bigelow, D.S., Slusser, J.R., Beaubien, A.F. and Gibson, J.H., "The USDA ultraviolet radiation monitoring program", *Bull. Am. Met. Soc.* (1998), **79**(4), 601-615.

9. Rosales, A., Pedroni, J.V. and Tocho, J.O., “Global spectral UV-radiometer with automatic shadow band”, *Photochem. Photobiol.* (2006), **82**, 844-849.
10. Grant, R.H., “Shadow-band corrections for photosynthetically-active radiation under clear and overcast conditions”, *Agr. For. Meteor.* (1997), **87**, 213-222.
11. Huber, M., Blumthaler, M., Ambach, W. and Staehelin, J., “Total atmospheric ozone determined from spectral measurements of direct solar UV irradiance”, *Geophys. Res. Lett.* (1995), **22**(1), 53-56.
12. Grant, R.H. and Gao, W., “Diffuse fraction of UV radiation under partly cloudy skies as defined by the Automated Surface Observation System (ASOS)”, *J. Geophys. Res.* (2003), **108**(D2), 4046, doi:10.1029/2002JD002201.
13. ACCV (Anti-Cancer Council of Victoria), *SunSmart Campaign 2000-03*, Report of the Anti-Cancer Council, Melbourne, (1999).
14. DAUQ, Department of Architecture, University of Queensland, *Shade for sports fields*, Brisbane, Queensland Health, (1995).
15. DAUQ, Department of Architecture, University of Queensland, *Shade for public pools*, Brisbane, Queensland Health, (1996).
16. DAUQ, Department of Architecture, University of Queensland, *Shade for young children*, Brisbane, Queensland Health, (1997).
17. Greenwood, J. Designing sun safe environments, *UV Radiation and its Effects: an update (2002) Conference*, Christchurch, New Zealand, 26-28 Mar, (2002).
18. Gies, P. and Mackay, C., “Measurements of the solar UVR protection provided by shade structures in New Zealand primary schools”, *Photochem. Photobiol*. (2004), **80**, 334-339.
19. Turnbull, D.J. and Parisi, A.V., “Effective shade structures”, *Med. J. Aust.* (2006), **184**, 13-15.

20. Kollias, N., Baqer, A.H. and Ou-Yang, H., “Diurnal and seasonal variations of the UV cut-off wavelength and most erythemally effective wavelength of solar spectra”, *Photodermatol. Photoimmunol. Photomed*. (2003), **19**, 89-92.

21. Parisi, A.V. and Turner, J., “Variations in the short wavelength cut-off of the solar UV spectra for cataracts”, *Photochem. Photobiol. Sci.* (2006), **5**, 331–335.

22. Parisi, A.V. and Downs, N., “Cloud cover and horizontal plane eye damaging solar UV exposures”, *Int. J. Biomet*. (2004), **49**, 130-136.

23. Sabburg, J. M. and Parisi, A.V., “Spectral dependency of cloud enhanced UV irradiance”, *Atmospheric Research*, (2006), **81**, 206-214.

24. Kylling, A., Albold, A., Seckmeyer, G., “Transmittance of a cloud is wavelength-dependent in the UV range: Physics Interpretation” *Geophys. Res. Lett.* (1997) **24**(4), 397-400.

25. TOMS, Total Ozone Mapping Spectrometer, NASA (2007) Data Product: Ozone. Available at: http://toms.gsfc.nasa.gov/ozone/ozone_v8.html. Accessed March 2007

Figure Captions

Figure 1 – The configuration of the input optics of the spectroradiometer with the diffuse shadow band in position for the recording of a diffuse UV spectrum.

Figure 2 - A typical diffuse UV solar spectrum (thin line) and associated global UV solar spectrum (thick line) for a SZA of 5.4^{o} (top graph) and the associated spectral erythemal UV for the diffuse UV and the global UV (bottom graph).

Figure 3 – The diffuse erythemal UV irradiances on (a) a cloudy day with cloud fractions up to 1 and (b) a cloud free day.

Figure 4 – Variation of the short wavelength cut-off for the diffuse erythemal UV with time of day on (a) a cloudy day and (b) a cloud free day.

Figure 5 – The variation with SZA of the cut-off wavelengths for the diffuse erythemal UV for (a) all sky conditions and (b) cloud-free conditions. Each data point is the average over the four months of the data that are 5^{o} either side of the data point.

Figure 6 – The variation with SZA of the wavelength at which the maximum irradiance occurs for the diffuse erythemal UV. Each data point is the average over the four months of the data that are 5^{o} either side of the data point.

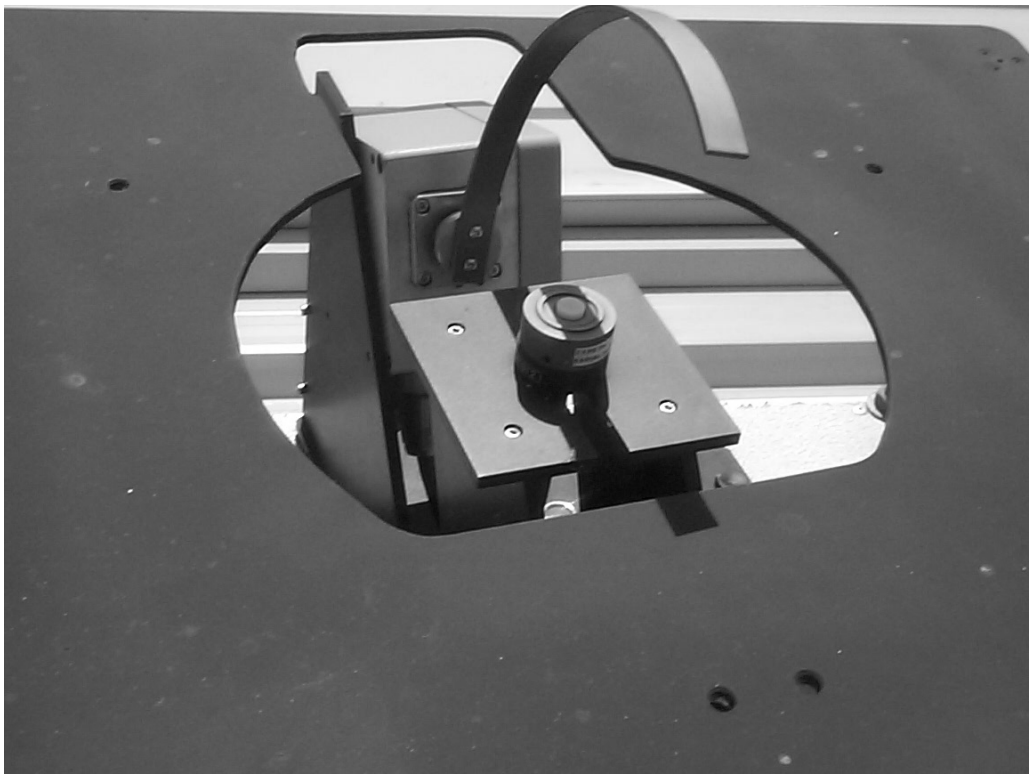

Figure 1 – The configuration of the input optics of the spectroradiometer with the diffuse shadow band in position for the recording of a diffuse UV spectrum.

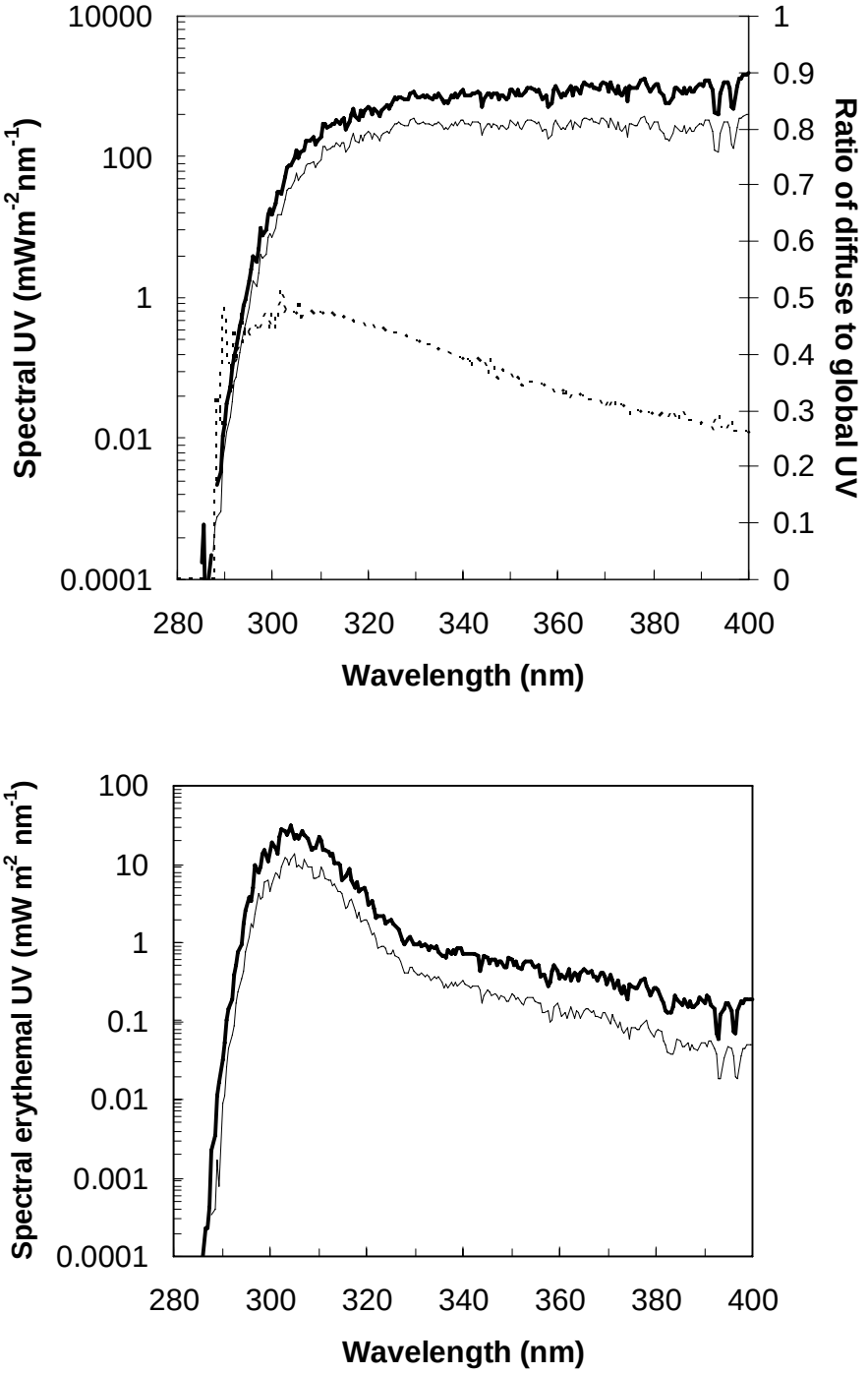

Figure 2 - A typical diffuse UV solar spectrum (thin line), associated global UV solar spectrum (thick line) and ratio of diffuse UV to global UV (dashed line) for a SZA of 5.4^{o} (top graph) and the associated spectral erythemal UV for the diffuse UV and the global UV (bottom graph).

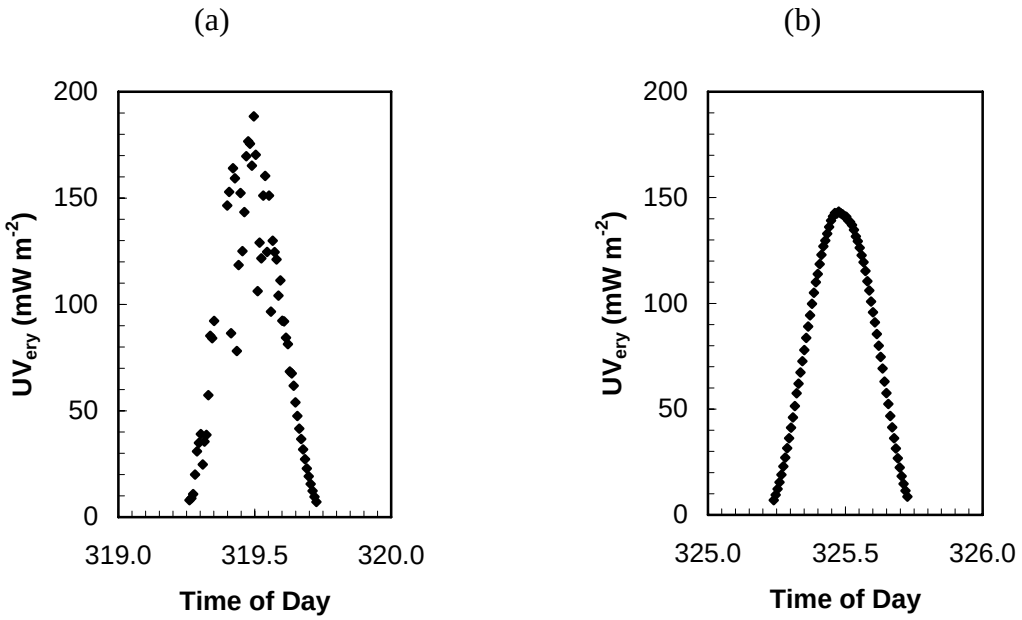

Figure 3 – The diffuse erythemal UV irradiances on (a) a cloudy day with cloud fractions up to 1 and (b) a cloud free day.

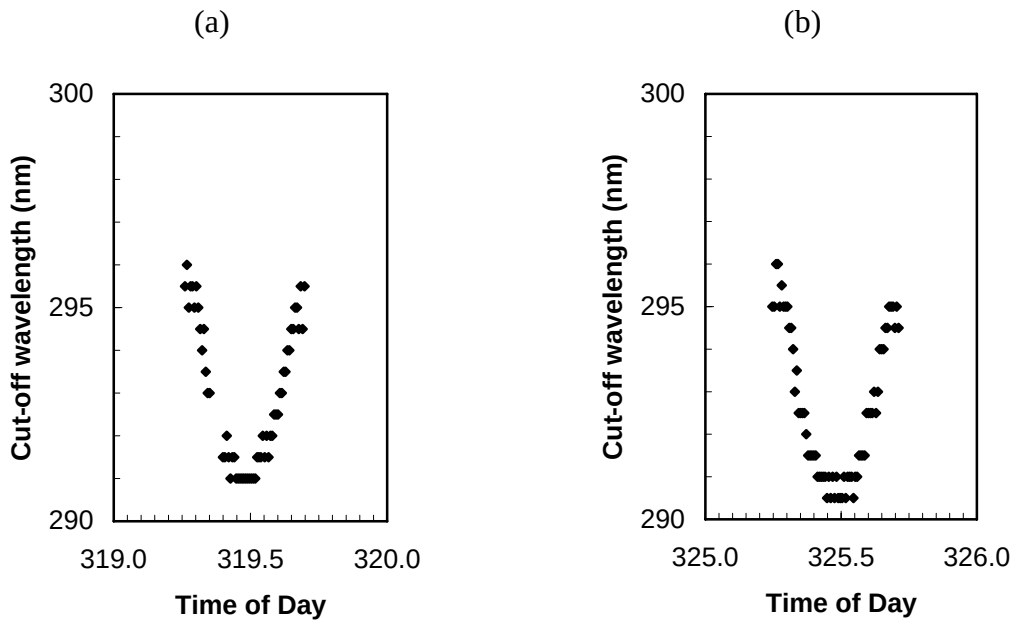

Figure 4 – Variation of the short wavelength cut-off for the diffuse erythemal UV with time of day on (a) a cloudy day and (b) a cloud free day.

(a)

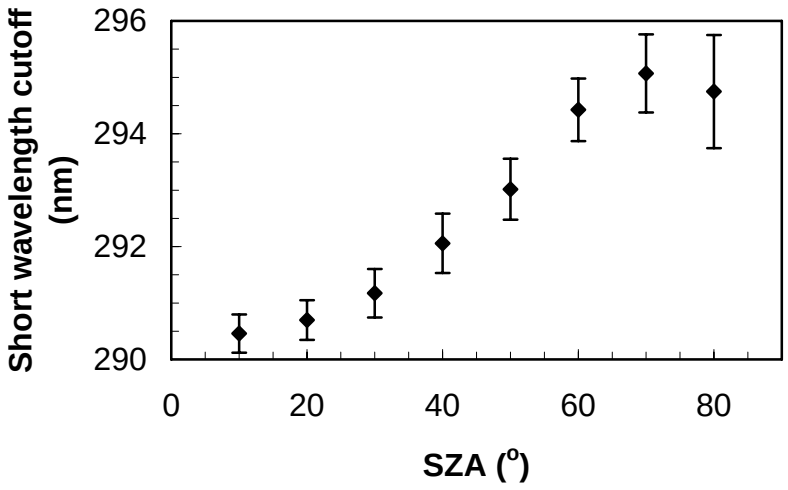

(b)

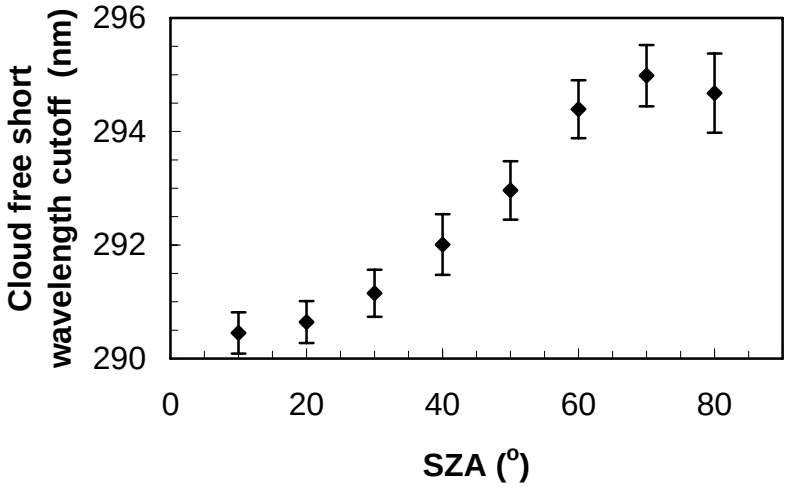

Figure 5 - The variation with SZA of the cut-off wavelengths for the diffuse erythemal UV for (a) all sky conditions and (b) cloud-free conditions. Each data point is the average over the four months of the data that are 5° either side of the data point.

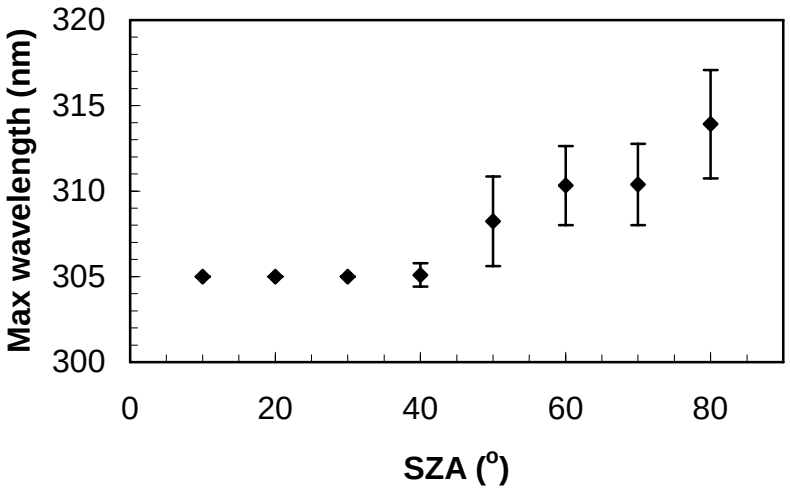

Figure 6 - The variation with SZA of the wavelength at which the maximum irradiance occurs for the diffuse erythemal UV. Each data point is the average over the four months of the data that are 5^{o} either side of the data point.